Development and functionalization of magnetic nanomaterials for biomedicine applications

Thais Sayuri Berberich

Final dissertation submitted to Escola Superior de Tecnologia e Gestão of Instituto Politécnico de Bragança to obtain the Master's Degree in Chemical Engineering in the ambit of the double diploma with the Universidade Tecnológica Federal do Paraná.

Escola Superior de Tecnologia e Gestão

Instituto Politécnico de Bragança

Supervisor:

Dr. Helder T. Gomes (IPB)

Co-supervisors:

Dr. Jose L. Diaz de Tuesta (IPB)

Drª. Simone Delezuk Inglez (UTFPR)

Bragança

March/2020

Acknowledgements

Many people have facilitated the preparation of this work for both practical and scientific support, as well as in an emotional and affective way. In this sense, I extend my acknowledgements to all who have been with me throughout this research, in special to my parents and my friends.

I thank the professors Dr. Helder T. Gomes, Dr. Jose L. Diaz de Tuesta and Drª. Simone Delezuk Inglez for the scientific support and guidance in the project, as well as the encouragement of the academic career.

Also, I gratefully appreciate for the financial support of Project "RTChip4Theranostics - Real time Liver-on-a-chip platform with integrated micro(bio)sensors for preclinical validation of graphene-based magnetic nanocarriers towards cancer theranostics", with the reference NORTE-01-0145-FEDER-029394, supported by Norte Portugal Regional Operational Programme (NORTE 2020), under the Portugal 2020 Partnership Agreement, through the European Regional Development Fund (ERDF); and CIMO - UIDB/00690/2020 - funded by Foundation for Science and Technology (FCT, Portugal) and FEDER under Programme PT2020

Abstract

During the past decade, researchers have shown an increased interest in multifunctional nanomaterials. Magnetic Nanoparticles (MNP) have been one of the most attractive types of nanomaterials used in different fields, as in environmental protection and biomedical applications. These applications include drug delivery, magnetic resonance imaging, magnetic hyperthermia, among others. MNPs have been synthesized by various methods. Amongst the most common may be referred: thermal decomposition, microemulsion, coprecipitation, solution combustion and sonochemical synthesis.

The main objective of this MSc thesis is the development of biocompatible MNPs with high potential for the controlled release of drugs. For this purpose, a magnetic core based on magnetite is developed by two different approaches of Solution Combustion Synthesis. In the first approach, the synthesis of MNPs is obtained by reduction of Fe (III) using citric acid, and the in second approach, the MNPs are synthesized using tangerine peel extract for the reduction of Fe (III). However, the material produced with the extract was not magnetic, and it was decided to not continue the methodology with it. Then, the magnetic core, produced with citric acid, is coated with a resin prepared from formaldehyde, resorcinol and TEOS, which is later carbonized by pyrolysis at 600 ºC. Subsequently, the silica generated from TEOS is removed by etching with NaOH in order to create a void inside the particle, which take the known yolk-shell shape. Finally, the materials are functionalized with nitric acid and subsequent pluronic F-127, for its biocompatibility and dispersibility. These materials are then assessed in the controlled release of two different drugs to test the potential of the developed magnetic nanostructures for drug delivery applications: Doxorubicin (DOX) and Omeprazole (OME). Drug Loading Capacity and Efficiency of 0.936 $\mu g \cdot \mu g^{-1}$ and 93.6% for DOX and 0.335 $\mu g \cdot \mu g^{-1}$ and 33.5% for OME are obtained at pH 7.4, respectively. Finally, the drug release is tested at the pH of the normal tissue (pH 7.4) and at the pH of the extracellular environment of the tumor (pH < 6.5), simulating different circumstances of the human body.

Keywords: nanomaterials; magnetic; biomedicine; solution combustion synthesis; drug delivery.

Resumo

Durante a última década, os pesquisadores tem mostrado um interesse crescente em nanomateriais multifuncionais. As nanopartículas magnéticas (MNPs) tem surgido assim como um dos tipos de nanomateriais mais promissores para diversos fins, podendo ser utilizado, por exemplo, em proteção ambiental e em aplicações biomédicas. De entre estas aplicações podemos citar a libertação controlada de fármacos, a ressonância magnética, o tratamento hipertermia magnética, entre outros. As MNPs podem ser sintetizadas das mais diversas maneiras, entre as quais as mais comuns são: decomposição térmica, microemulsão, coprecipitação, síntese por combustão de solução e síntese sonoquimica.

O principal objetivo desta tese é desenvolver MNPs biocompatíveis com grande potencial para a libertação controlada de fármacos. Para isso, será produzido um núcleo magnético, feito de magnetite, considerando duas abordagem de síntese de combustão de solução. Na primeira abordagem, as MNPs são produzidas reduzindo o Fe (III) com ácido cítrico. Na segunda abordagem, o agente responsável pela redução dos iões de Fe (III) é um extrato de tangerina, porém utilizando esse agente o material produzido não era magnético, e optou-se por não continuar a metodologia com ele. Em seguida, o núcleo magnético, produzido com o ácido cítrico, é revestido com uma resina preparada a partir de formaldeído, resorcinol e TEOS, que posteriormente é carbonizada por pirólise a 600 ºC. Após a carbonização, a sílica gerada a partir de TEOS é removida com NaOH, a fim de criar um vazio no interior do material, que assume a forma conhecida como casca de gema. Finalmente, os materiais são funcionalizados com ácido nítrico e subsequente plurônico F-127, para obter características de biocompatibilidade e dispersibilidade. Os materiais sintetizados são então avaliados na libertação controlada de dois fármacos, para testar o potencial das nanoestruturas magnéticas nessa aplicação biomédica: Doxorrubicina (DOX) e Omeprazol (OME). Obteve-se uma capacidade de carga dos fármacos e uma eficiência de 0,936 $\mu g \cdot \mu g^{-1}$ e 93,6% para DOX e 0,335 $\mu g \cdot \mu g^{-1}$ e 33,5% para OME, respetivamente, obtidas a pH 7,4. Finalmente, a libertação do fármaco é testada no pH do tecido normal (pH 7,4) e no pH do ambiente extracelular do tumor (pH < 6,5), simulando diferentes circunstâncias do corpo humano.

Palavras-chave: nanomateriais; magnético; biomedicina; síntese de combustão de solução; libertação de fármacos.

Index of content

Index of figures

Index of tables

Index of abbreviations

CCYSMNP - Carbon-coated yolk-shell magnetic nanoparticles

CS - Core–shell

CSNPs - Core-shell nanoparticles

CYSMNPs - Carbon-based yolk-shell magnetic nanoparticles

DLC – Drug loading capacity

DLE – Drug loading efficiency

DOX - Doxorubicin

FeNps - Iron nanoparticles

FYCSMNP - Functionalized yolk carbon shell magnetic nanoparticles

GYSMNP - Graphene-based yolk-shell magnetic nanoparticles

MagN - Magnetite nanoparticle

MNPs - Magnetic nanoparticles

MRI - Magnetic resonance imaging

MRI - Magnetic resonance imaging

NCs - Nanocomposites

OME - Omeprazole

SCS - Solution combustion synthesis

TEOS – Tetraethyl orthosilicate

XRD – X-ray diffraction

YCSMNP – Yolk carbon shell magnetic nanoparticles

YS - Yolk-shell

YSNPs - Yolk-shell nanoparticles

Chapter 1: Introduction

1 Introduction

Magnetic nanoparticles (MNPs) have emerged as promising advanced functional materials for a wide field of potential applications, such as catalysis, water treatment, environmental remediation, biotechnology/biomedicine, magnetic recording media, electromagnetic wave absorption and magnetic sensors [1,2]. Multiple techniques have been developed to prepare iron nanoparticles, including thermal decomposition, sonochemical decomposition, vapor phase condensation and solution combustion [2]. In recent years, the synthesis by solution combustion has become a promising candidate for the preparation of a large variety of nanoparticles [3]. It is considered a time/energy saving methodology for the preparation of inorganic nanopowders with high reactivity and tailored defects [4]. In alternative to the traditional solution combustion synthesis with chemical reductants, green routes using plant extracts emerged as environmentally friendly ways to synthesize MNPs. Plant extracts are used to prepare MNPs, since there are no harmful agents to be discarded [5,6].

In this work, the synthesized nanoparticles will be used as magnetic cores, further coated with carbon in yolk-shell structures, with the carbon-based coating, in relation to other coatings, showing better chemical and physical properties [7]. In addition to the coating, carbon-based yolk-shell magnetic nanoparticles (CYSMNPs) will be functionalized with nitric acid, the resultant CYSMNPs becoming negatively charged and enabling them to have great affinity with cationic drugs, such as Doxorubicin and Omeprazole. The electronic affinity between the CYSMNPs and the drugs can be different in solutions with different pH. Such difference can facilitate both the drug loading and the drug release depending on the solution that will be used. However, due to this behavior, it is possible to study the optimization of the magnetic core production, coating and functionalization efficiency and the drug loading and release environment, focusing on the release of higher amount of drugs, simulating different conditions of the human body.

1.1 Objectives

The main objectives of this dissertation are the development and functionalization of magnetic nanostructures coated with carbon materials with high potential for the controlled release of drugs. The magnetic core is developed by two approaches of Solution Combustion Synthesis (SCS). In the first approach, the synthesis of the magnetic nanoparticles is done by the reduction of Fe (III) using citric acid. In the second approach, a green route is considered, using extracts of tangerine peel with high reducing power for the reduction of Fe (III). After the NPs synthesis and functionalization, the materials are applied in controlled drug release tests, using Doxorubicin (DOX) and Omeprazole (OME) as model drugs, under different conditions, mainly altering the pH of the medium in the range 4.0-7.4. Controlling the pH of the medium allow the drug to avoid side effects on normal cells.

Chapter 2: State of the Art

2 State of the Art

2.1 Magnetic Nanoparticles

Magnetic nanoparticles are systems formed by grains in the order of nanometers (10^{-9} m) and, due to its molecular and atomic state, they have physical and chemical properties quite different from those observed in bulky materials. The formation of magnetic monodomes, the existence of a large surface area in relation to the volume and the possibility to coat the nanoparticles with various types of specific binders, are some of the characteristics responsible for making MNPs potentially important in technological applications [8,9].

During the past decade, researchers have shown an increased interest in multifunctional nanomaterials. Analyzing the statistics at the Scopus database of the publications about "magnetic nanoparticles" over the last 10 years, more than 50 000 papers have been published. According to the Web of Science database, the number of citations per year has been linearly increasing, reaching 9 717 citations last year. MNPs have been one of the most attractive types of nanomaterials used in different fields [10]. The biomedical applications of MNPs have become prominent topics for researchers in the modern century. These applications include drug delivery, magnetic resonance imaging (MRI) and magnetic hyperthermia treatment, among others [11–13]. Also, MNPs can be very useful for environmental protection applications, water treatment, environmental remediation, biotechnology/biomedicine, magnetic recording media, electromagnetic wave absorption and magnetic sensors [2,14,15].

Two key issues dominate the magnetic properties of nanoparticles: finite-size effects and surface effects, which give rise to various special features [16]. They also exhibit a lot of important features, such as high specific surface area, chemical stability, low intraparticle diffusion rate, high loading capacity and superparamagnetism [17,18]. The performance of the magnetic materials is classified based on their response to an external magnetic field [7]. The magnetism can be categorized in three basic types: diamagnetism, paramagnetism and ferromagnetism [1].

Magnetic nanoparticles prepared from iron oxide are considered attractive due to their multifunctional characteristics, including small size, supermagnetism and low toxicity. They are responsive to the application of a magnetic field [19,20] and, in this way, the substances to which they are complexed can be manipulated and transported [19].

The main challenge when using magnetic nanoparticles is the agglomeration of the nanoparticles when they are subjected to an internal or external magnetic field. In order to overcome that inconvenience, it has been necessary to coat the magnetic nanoparticles with an inert shell, which modify their surface properties and prevent direct contact between them. Magnetic nanoparticles coated with a polymer or an inorganic nanostructure have been widely studied because of their unique properties [21,22].

2.2 Iron Oxides

Hematite (α-Fe_2O_3), magnetite (Fe_3O_4) and maghemite (γ- Fe_2O_3) are three of the most important iron oxides used in various technological applications [23,24]. In particular, magnetite and maghemite possess some physicochemical properties such as low toxicity, biocompatibility and high surface area, making them convenient for applications in several areas including catalysis/photocatalysis, magnetic storage media, magnetic fluids, biomedicine or electrochemical applications [23,25,26].

Comparing all kinds of magnetic oxides, magnetite nanoparticles (MagN) are considered as the most promising, due to its excellent magnetic properties. This is notably important in biomedical applications, since the materials demand a high standard of stability and nontoxicity in addition to hydrophilic properties [14]. Magnetite and magnetite colloids have low toxicity, good biocompatibility and tunable magnetic properties. Fe_3O_4 microcrystals have different morphologies depending on the pH values of the precursor solution [27].

Another interesting property of magnetite is its superparamagnetic behavior, i.e. the capacity of the nanoparticles to become strongly magnetic in the presence of a magnetic field and, when the field is removed, to become immediately re-dispersed in solution, because do not show any residual magnetism [28].

2.3 Nanocomposites

Nanocomposites (NCs) are multi-phasic materials with a matrix material that incorporates units with at least one dimension in the size range below 100 nm, resulting in novel functional materials [29]. The characteristics of nanocomposites depends on its constituent materials, size, structure and formation, and it can exhibit different properties from its

individual constituent materials and also from its bulk form [30]. Nanocomposite structures containing metals and semiconductors are expected to have important practical applications due to the fact that they exhibit surface plasmonic and excitonic resonance [31,32].

One of the major challenges in the synthesis of nanocomposites is how to produce the desired structure with various functions such as catalytic, magnetic, electronic and optical properties, as well as surface functionality coupled with biocompatibility, low toxicity and high stability. Magnetic nanocomposites with magnetic cores and functional shells have drawn the attention because of their unique functionality and separability [33].

The use of coatings, like polymers, silica, carbon or other materials, over the magnetic particles can stabilize them, preventing aggregation and functionalizing the MNPs to extend their applications [34]. Nowadays, nanocomposites are employed in multiple technological fields, such as electronics, optics, medical fields, materials modification and many other fields [29,31].

2.4 Methods of Synthesis

There have been impressive developments in the field of nanotechnology with numerous methodologies formulated to synthesize nanoparticles [6]. There are some popular ways to achieve shape-controllable, monodisperse and highly stable MNPs, such as solution combustion synthesis, co-precipitation, hydrothermal synthesis, thermal decomposition, microemulsion, sonolysis and biosynthesis [17] .

Co-precipitation is a facile and convenient way to synthesize iron oxides from aqueous Fe^{2+}/Fe^{3+} solutions, by the addition of a base at room temperature or at an elevated temperature. The size and shape of the magnetic nanoparticles depends very much on the type of salts used [16,17,35].

Magnetic nanocrystals can essentially be synthesized through the thermal decomposition of organometallic compounds, such as metalacetylacetonates, metal cupferronates or carbonyls, in high-boiling organic solvents containing stabilizing surfactants. Fatty acids, oleic acid, and hexadecylamine are often used as surfactants. The shape and size of the nanoparticles depend on the proportion of organometallic precursors, surfactants and solvents [16,17].

Microemulsions are isotropic, thermodynamically stable and colloidal dispersions, consisting of at least three components: a non-polar phase, a polar phase and a surfactant [36]. In this method, the hydrocarbon phase is continuous and the aqueous phase is dispersed as microsphere, which is surrounded by the singer-layer surfactant molecules. The size of the reverse micelle depends on the molar ratio of surfactant to water. Using the microemulsion technique, metallic cobalt, cobalt/platinum alloys and gold-coated cobalt/platinum nanoparticles have been synthesized in reverse micelles of cetyltrimethlyammonium bromide, using 1-butanol as the cosurfactant and octane as the oil phase [16,17].

The hydrothermal synthesis is usually applied in aqueous media in reaction kettles at high pressure and high temperature, involving the hydrolysis and condensation of the metal salt, in the presence of water, to produce ultrafine metal oxides or metal particles, with magnetic properties [37]. Hydrothermal processing is one of the successful ways to grow crystals of many different materials. This technique has also been used to grow dislocation free single crystal particles and grains formed in this process could have a better crystallinity than those from other processes [16,17,35]

For the sonolysis method, new structures can be produced through high intensity ultrasound, and it has no need for high pressure, high temperature or long time of reaction, which make it an unusual route. The sonolysis technique involves passing sound waves of fixed frequency through a slurry or solution of carefully selected metal complex precursors [38]. As a result, the sonolysis method is usually applied to achieve different types of bare and functionalized nanoparticles [17,35].

Biosynthesis involve the use of green technology, such as crude extracts from plants, that are responsible for the reduction process of metal ions in the redox reaction to obtain nano-sized nontoxic particles. The exact mechanism of the biosynthesis has not been explained clearly, and the shape and size of the nanoparticles can’t be controlled precisely [17,39,40].

2.4.1 Solution Combustion Synthesis

Among the soft chemical methods, the SCS is an efficient method for the preparation of oxide materials. Moreover, it is considered as a potential route for the preparation of iron oxide composites. It is essentially a self-sustained exothermic redox reaction between an oxidizer and a fuel in a homogenous aqueous solution. Usually, oxidants are metal precursors

themselves, like for example metal nitrates, sulfates and carbonates, and the fuel is any organic material, as for example citric acid, urea and glycine [2,41]. Among various metal salts, hydrated nitrates are preferred as metal precursors, because of the efficient oxidizing power of NO_3^- groups, and their lower decomposition temperature and good solubility in water [41]. Basically, the SCS consists of three main steps, specifically the formation of the combustion mixture, the formation of the gel and the combustion of the gel [4].

The main advantage of the SCS is its time- and energy-efficiency, with low costs of the raw materials, simplicity, short reaction time and low energy consumption of the synthesis method [4,23,41]. In addition to these advantages, the SCS only needs simple and low cost instrumentation that can be easily scaled up, and it has the possibility to obtain products with diverse functionality and structures [41].

The final products obtained through SCS are materials with high purity, high surface area, optimum agglomeration, high adsorption capacity for both anionic and cationic dyes, short time to reach equilibrium, good potential of regeneration and reuse and environmentally friendly [4,23,42].

2.4.2 Solution Combustion Synthesis with plant extracts

The conventional way to synthesize Iron Nanoparticles (FeNps) use a variety of organic solvents and reducing agents like sodium borohydride ($NaBH_4$), hydrazine and sodium dodecyl sulphate, among others [43]. These reducing agents can cause risks to the environment and can create harmful by-products to human health [44]. Green synthesis is an alternative way to synthesize MNPs. Normally, this type of synthesis is made by adding only plant extracts in a solution containing Fe(III) and/or Fe(II) [45]. The nanoparticles synthesized using such green technologies have diverse natures, with higher stability and appropriate dimensions [46].

The use of plant extracts gives the possibility to prepare magnetic nanostructured materials via several chemical routes, using benign reagents, thus reducing the risk of using dangerous substances [47]. For the SCS, the plant extracts will act like a fuel in the chemical reaction [5]. This approach for the SCS, can influence the nanoparticles that are produced, like their size, shape and morphology. In addition, this method also generates nanoparticles with high dispersibility and high stability [47].

2.5 Structure of Nanocomposites

Depending on the type of synthesis used, the composition and their purpose, the structure of nanocomposites can change from each other [7]. Based on their form, the nanocomposites can be divided in distinguished categories, as solid nanoparticles, Janus particles, hollow particles, core–shell (CS) particles and reverse bumpy balls and yolk-shell (YS) particles [48]. Figure ***1*** show those types of structure.

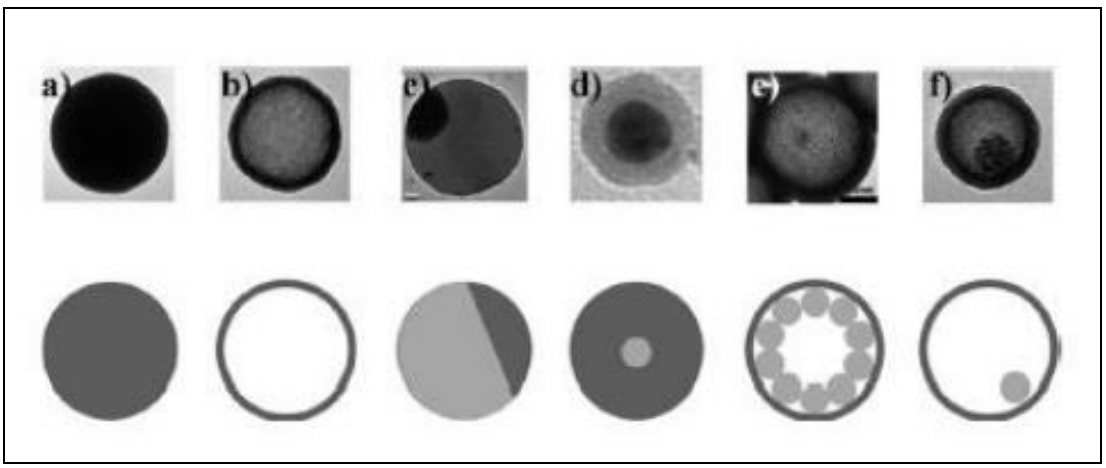

Figure 1 - Transmission Electron Microscopy (TEM) images and schematic representations of the common types of nanostructures: a) Solid nanoparticle, b) Hollow particle, c) Janus particle, d) Core-shell particle, e) Reverse bumpy balls and f) Yolk-shell particle [48].

It is important to know the differences between those types of nanostructures. Solid nanoparticles are composed by one or many elements, but with a uniform structure. In Janus particles, the two parts of the particle have different chemical or physical properties. The Hollow particles have an empty interior. The core-shell type have comprising smaller solid particle(s) coated with a tight layer of other element(s), as well as from reverse Bumpy balls which have encapsulated cores attached to the shell [48].

Sometimes, issues of biocompatibility and toxicity limit the choice of the materials. However, the use of coatings may make the use of these materials feasible. This process also decrease the agglomeration of particles [1]. The coating can be polymeric or based on activated carbon, silica and gold, among other materials. The coating can be separated in two categories: organic components coating and the inorganic components coating. The organics include polymers and surfactants that can be added to the surface of the nanoparticles during

or after the synthesis to avoid aggregation. The inorganics includes carbon, silica, precious metals or oxides. Carbon coatings are used to protect magnetic nanoparticles because this type of coating materials have higher thermal stability and higher biocompatibility than polymers or silica. The most applied coated structures are core-shell and yolk-shell [17,29,30]. Also, the use of some reagents in the synthesis of the coating, as Tetraethyl Orthosilicate (TEOS), helps to control the distribution of MNPs. The surface coating of MNPs is carried out to control the size, the shape, the dispersibility of the nanoparticles in the solvent and to develop the effective protections to maintain the stability of the nanoparticles [49]. In this case, TEOS was chosen in this work, since it hydrolyses in the presence of water, generating silanol groups (Si-OH) that polymerize to form siloxane bonds (Si-O-Si) and ultimately inducing the precipitation of a silica gel [50]. In addition, the shell can be constituted by multiple layers and contain functional groups or targeting moieties [48]. For this work, it was chosen to coat the MNPs by polymerization of resorcinol and formaldehyde (RF).

In a first step of the coating process, silica spheres are produced. Ammonia is used to prevent the particles aggregation and to allow the formation of a stable colloidal suspension. In parallel to the formation of the silica spheres a slower reaction occurs between resorcinol and formaldehyde catalyzed by OH^- ions. Condensation between these species will occur within the nanospace surrounding the silica particles resulting in the formation of a RF polymeric layer around the silica spheres. To produce the carbon coating, the nanoparticles are then heated in nitrogen atmosphere to convert the RF polymeric layer into carbon. Subsequently, the carbonized product formed is washed with sodium hydroxide to dissolve the silica core [51].

Normally, after the coating process, the shell is functionalized for a best performance in the desired application. This functionalization can be made using Pluronic-127. The use of Pluronic F-127 aims to enhance the colloidal stabilization and biocompatibility of the GYSMNPs [52].

2.5.1 Core shell

Core-shell nanoparticles (CSNPs) are a class of particles containing a core and a shell. The core and the shell can be different materials or the same materials with different structures. The core may be a single sphere or an aggregation of several small spheres. The

shell structure can be a continuous layer or the attachment of smaller spheres onto a bigger core sphere or aggregated core spheres [53].

The process to synthesize core–shell particles are usually a two-step or a multiple-step process. The core is synthesized first and the shell is then formed on the core particle via different methods, depending on the type of core and shell materials and on their morphologies [53]. The motivation in the preparation of core-shell particles is to combine the desired properties of different materials and structures in order to offer simultaneous effects, to stabilize the active particles or to provide biocompatible properties [7].

In the case of magnetic nanocomposites with core-shell structures, their magnetic properties are sometimes restrained to a specific range, since the core materials are easily and compactly encapsulated in the shell material [13].

2.5.2 Yolk shell

The yolk-shell nanoparticles (YSNPs) represent a new class of special core-shell structures with a distinctive core@void@shell configuration, generally denoted as A@B [54]. The main difference between the CSNPs and the YSNPs is the presence of a void space derived from the sacrificial layer, which gives rise to multifunctional and other unique properties of YSNPs [7]. The YSNPs are defined as hybrid structures (mixture of core/shell and hollow) where a core particle is encapsulated inside the hollow shell and may move freely inside the shell. For that reason, they are also termed as movable core/shell or rattle-type nanostructures [55].

YSNPs are functional nanomaterials with multiple applications, such as catalysis, nanoreactors, drug/gene delivery, lithium-ion batteries and biosensors, achieved due to their tailorability and functionality in both the cores and hollow shells [54]. So far, researchers have synthesized four types of yolk-shell nanoparticles, specifically those with single cores, multiple cores, multiple shells and raspberry-like cores [13].

According to the core and shell morphologies, YSNPs can be classified into ‘spherical’ and ‘non-spherical’ structures. The spherical structures have the core and the shell in a spherical shape, and in the ‘non-spherical’ structure at least one structure should be non-spherical [55].

The synthesis of YSNP usually involves several steps including the fabrication of the core, the growth of the shell, as well as various post-synthesis treatments, such as core removal, functionalization of compartments and loading with cargo [48]. Commonly, the synthesis starts with the formation of the core (or yolk) of the structure, followed by coating with the desired material according to the application of the synthesized NPs [7].

2.6 Applications

Magnetic nanoparticles are of great interest for a wide range of areas, such as catalysis applications, industrial applications, drug delivery, bioseparation, environmental applications and magnetic hyperthermia treatment. There are still a wider range of applications for the magnetic nanoparticles, which requires advances in the techniques in order to produce nanoparticles with specific sizes and well controlled magnetic properties. The application of magnetic nanoparticles also highly depends on the stability of the particles [16,20].

2.6.1 Industrial Applications

Magnetic iron oxides are commonly used as synthetic pigments in paints, ceramics and porcelain, because they display a range of colors with pure hues and high tinting strength [24]. Magnetite and hematite have been used as catalysts for a number of industrially important reactions, including the synthesis of NH_3. They can also be applied in many areas including high density magnetic data storage devices, magnetic information storage, xerography, electronics (recording media), catalysis, magnetic inks (for jet printing) and magnetic refrigeration and their systems, among others [35,56,57].

2.6.2 Bioseparation

In biomedical research, the separation of specific biological entities from their native environment is sometimes required. Superparamagnetic colloids are ideal for this application due to their on-off nature of magnetization, with and without an external magnetic field, enabling the transportation of biomaterials with a magnetic field [35]. Magnetic nanoparticles have been extensively used for separation and purification of cells and biomolecules in bioprocesses [35,58,59].

2.6.3 Drug Delivery

The possibilities for the application of magnetic nanoparticles in drug targeting have drastically increased in the last few years [16]. MNPs, in combination with an external magnetic field and/or magnetizable implants, allow the delivery of particles to the desired target area and their fixation at the local site, while the medication is released and acts locally. In other words, the magnetic particles first acts as carriers of the drug, which is attached to its outer surface. Once the drug-coated particles have been introduced into the bloodstream of the patient, a magnetic field gradient is used to guide the particles to the targeted region. This kind of treatment can eliminate side effects and also reduce the required dosage [35,60].

2.6.4 Catalysis Applications

The recovery of catalysts in a liquid-phase reaction can be much easier using a magnetically driven separation, when compared to a cross flow filtration and centrifugation, especially when the catalysts are in the sub-micrometer size range. In terms of recycling expensive catalysts or ligands, immobilization of these active species on MNPs leads to the easy separation of catalysts in a quasi-homogeneous system [16,35]. Magnetic nanoparticles with core–shell structure may enable the development of a new type of catalysts, in which the shell consists of the catalytically active species, and the magnetic core can act as anchor to separate and recycle the catalyst [16].

2.6.5 Environmental Applications

For environmental applications, nanotechnology offers the potential of novel functional materials, processes and devices with unique activity toward recalcitrant contaminants, enhanced mobility in environmental media and desired application flexibility [61]. Iron NPs technology is considered to be among the first generation of nanoscale environmental technologies, which could provide cost-effective solutions to some of the most challenging environmental cleanup problems [35,62]. Extensive laboratory studies have demonstrated that nanoscale iron particles are effective for the transformation of a wide array of common environmental contaminants, such as chlorinated organic solvents, organochlorine

pesticides, PCBs, organic dyes, various inorganic compounds and metal ions such as As(III), Pb(II), Cu(II), Ni(II) and Cr(VI) [61].

2.6.6 Magnetic hyperthermia Treatment

Another interesting application of magnetic nanoparticles is in magnetic hyperthermia treatment, as a supplementary treatment to chemotherapy and radiotherapy. Magnetic hyperthermia employs magnetic nanoparticles as heat sources to raise tissue temperature to ~43°C, based on the fact that when magnetic nanoparticles are exposed to a varying magnetic field, heat is generated by the magnetic hysteresis loss, at which tumors cells are known to be more sensitive to heat than healthy cells. The localization of the MNPs is obviously critical to the success of hyperthermia as the objective is to spare the surrounding healthy tissue from excessive heat [16,17,20].

2.6.7 Magnetic Resonance Imaging

Magnetic nanoparticles have been studied as contrast agents in magnetic resonance imaging (MRI) for very promising applications, such as tumor imaging, cell labelling and tissue engineering [63,64]. Magnetite iron oxide nanoparticles are the most commonly used negative MRI contrast agents due to their magnetism, low toxicity and good biocompatibility compared to other MNPs (such as $MnFe_2O_4$ and $ZnFe_2O_4$). Nevertheless, specific narrow size distribution, superparamagnetic behavior and surface modification are needed properties in the nanoparticles for this application [65].

2.7 Drug Delivery

Targeted drug delivery to specific body parts has become one of the important ventures of today's world, as conventional dosage forms are generally associated with difficulties in approaching the target site with a specified dose after or during a proper time period. As a result, the development and evaluation of novel drug delivery systems has become more demanding in recent years [66]. The use of nanotechnology for this purpose has been promising, given the side effects of treatments such as chemotherapy and radiotherapy and the risks of surgeries for the patients [7]. NPs with diameters ranging from 10 to 200 nm

present promising pharmacokinetic features. Drug encapsulated NPs accumulate both passive and active mechanisms for extended and complete circulation periods, continuous drug discharge kinetics and recovery of tissues from tumor [67].

Nanotechnology is an emerging field of research that plays a key role in medicine, particularly in the formulation and delivery of drugs at pathological sites with increased success. The discovery of non-biodegradable NPs, including magnetic NPs, as coating agents in nano-drug delivery, has improved delivery at lower doses and increased aqueous solubility and bioavailability of the drug with reduced side effects. NPs can also increase a drug's circulation half-life period with advanced pharmacokinetics [68,69].

There are some important nanoparticle characteristics for drug delivery, such as particle size, surface properties of the nanoparticles, drug loading and drug release. Particle size and size distribution are the most important characteristics of nanoparticles, since they can influence drug loading, drug release and the stability of the nanoparticles. For example, smaller particles have a larger surface area-to-volume ratio; therefore, most of the drug associated with small particles would be at or near the particle surface, leading to faster drug release [70–72].

A successful nano-particulate delivery system should have a high drug-loading capacity, thereby reducing the quantity of matrix materials for administration. A drug can be loaded into the nanoparticle system by the following two methods: (i) drug integration during the process of production of the nanoparticles or (ii) drug adsorption after the synthesis of the nanoparticles. Additionally, it is important to consider both drug release and polymer biodegradation when developing a nano-particulate delivery system [72,73]. In this work, the drugs will be loaded after the synthesis of the nanostructures, since in the second step of the coating process the nanostructures are subjected to high temperatures, which could damage the dug.

Thus, the advantages of using nanoparticles for drug delivery are a result of main basic properties, due to their small size, enabling extravasation through the endothelium in inflammatory sites, epithelium and tumors or penetration in micro capillaries. Nanoparticles also have as advantage over larger micro particles the fact that they are better suited for intravenous delivery [72]. Also, they have an easy manipulation of particle size and its surface characteristics to achieve drug targeting, controlled and sustained discharge of the drug, both during the transportation and at the target site, high drug loading capacity, usage of various routes of administration, including parenteral, intra-ocular, oral, nasal etc. Efficient curcumin

delivery using nanotechnology, not only helps to overcome solubility, rapid drug metabolism, degradation and drug stability issues, but also should diffuse or target indent tissues while minimizing unintended toxicity to surrounding normal cells/tissues [69]. To achieve an increase of success in drug targeting, NPs can be coated with polymers, metals or non-metals [72].

Omeprazole is a synthetic molecule (345 Da) and a member of the group of pharmacological proton pump retardants, which play an essential role in controlling stomach acid production in humans by suppressing the proton pump in the stomach. It also has hormone-like functions that modulate natural hormone-signaling networks [74,75]. The chemical structure of Omeprazole is shown in Figure 2.

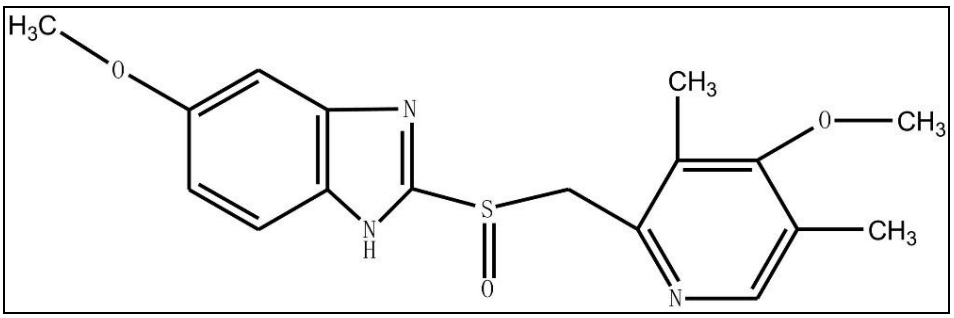

Figure 2- Chemical structure of Omeprazole [76]

Omeprazole is widely used in the treatment of active duodenal ulcer, active benign gastric ulcer, gastro-oesophageal reflux disease, erosive oesophagitis and other pathological hypersecretory conditions, such as Zollinger-Ellison syndrome [77]. Omeprazole is also very sensitive to light, heat, moisture, solvents and exposure to various salts and metal ions, which make it an excellent candidate as a worst-case study to develop multiple-coated particles [77,78].

Doxorubicin (DOX) is an anthracycline antiblastic antibiotic isolated from cultures of Streptomyces peucetius var. caesius. The chemical structure of DOX is shown in Figure 3. It is soluble in water for injections and in physiological saline solution [7]. Doxorubicin has been used in oncologic practice since the late 1960s. It held promise as a powerful drug in the fight against cancer, regression in various neoplasms, such as breast cancer, lung, bladder, thyroid and ovary carcinoma, soft tissue sarcoma and bone sarcoma, Hodgkin's and non-Hodgkin's lymphomas, neuroblastoma, Wilms' tumor, acute lymphoblastic leukemia and acute myeloblastic leukemia [79,80].

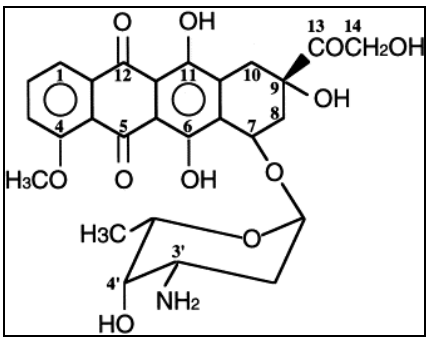

Figure 3 - Chemical structure of Doxorubicin [81]

Chapter 3: Methodology

3 Methodology

3.1 Reagents

For the synthesis of the magnetic core, a solution with iron (III) nitrate nonahydrate (Sigma-Aldrich, Germany) was used as iron source for magnetite formation and citric acid monohydrate (98.8%, WWR Chemicals, Belgium) and tangerine extract as the fuel of the SCS reaction. In the early stages of the coating reaction, the previously synthesized MNPs were dispersed in absolute ethanol (Carlo Erba, France) and distilled water, and the hydrolysis and condensation polymerization of TEOS (98% Fluka Chemika, Germany) was favored. Subsequently, as the reaction progressed and the TEOS hydrolysis and polymerization processes approached completion, the polymerization of resorcinol (99%, Fisher Scientific, U.K.) and formaldehyde (37-38% p/p, Panreac, Spain) became the predominant process, resulting in the formation of a phenolic resin polymer layer. To remove the silica, a sodium hydroxide solution (99.1 %, Fisher Scientific, U.K.) was used. The phosphate buffer solutions employed for drug loading and release were prepared with potassium dihydrogen phosphate (V.P., Portugal), disodium hydrogen phosphate 12-hydrate (Pronalab, Portugal), and sodium dihydrogen phosphate hydrate (Pronalab, Portugal).

3.2 Synthesis of functionalized carbon-coated magnetic nanoparticles

For a better understanding, the entire process can be divided in the following steps:

Step 1 – Synthesis of magnetite:

1.1 – SCS with citric acid.

1.2 – SCS with tangerine extract

Step 2 – Coating and carbonization under a N_2 atmosphere

Step 3 – Silica removal (etching)

Step 4 – Chemical treatment with nitric acid (HNO_3) 1 M

Step 5 – Functionalization with Pluronic F- 127

3.2.1 Synthesis of the magnetic core

The methodology to produce the magnetic core chosen in this work was the SCS, using iron (III) nitrate nonehydrate ($Fe(NO_3)_3 \cdot 9H2O$) as the oxidizer and citric acid ($C_6H_8O_7$) as the fuel of the reaction, as shown in the reaction Equation 1.

$$54\ Fe(NO_3)_3 + 46\ C_6H_8O_7 \rightarrow 18\ Fe_3O_4 + 276\ CO_2 + 184\ H_2O + 81\ N_2 \quad (1)$$

3.2.1.1 Production with citric acid

The magnetic core was synthesized using approximately 5.234 g of iron III nitrate nonahydrate ($Fe(NO_3)_3 \cdot 9H2O$), solubilized in 10 mL of distilled water in a 250 mL round bottom flask, to which 2.3198 g of citric acid ($C_6H_8O_7$), also solubilized in 10 mL of distilled water, was added dropwise using a peristaltic pump ISM 845, ISMATEC (Figure I - Annex A). The solution was heated at 80 °C in a drying oven, Binder FD 115 (Figure II- Annex A), for 6.5 h. The flask was placed in an oil bath heated by a magnetic stirring plate (IKA® C-MAG HS 7, Figure III - Annex A) and submitted to a flow of N_2 (100 $Ncm^3.min^{-1}$) for 1 h at 25 °C to ensure an inert atmosphere therein. After this time, the solution was heated to 180 °C for 3 h. Then, the product obtained was washed with distilled water until neutral pH, by centrifugation at 600 rpm during 5 minutes in a MPW- 260R centrifuge, MPW Med. Instruments (Figure IV - Annex A). The resultant material was dried in oven overnight at 60 °C.

3.2.1.2 Production with tangerine extract

For the production of the extract, peels of tangerines were used. The peels were dried by exposition to sun for 72 h and then placed in oven at a temperature of 100 °C for approximately 18 h. After drying, the peels were ground in an analytical mill, IKA

A11 basic (Figure V - Annex A) and particles with diameters between 250 and 106 μm were selected with sieves and stored in vial until their use.

The extract was obtained mixing 10 g of peels in 65 mL of distilled water under vigorous stirring in a 250 mL round bottom flask immersed in an oil bath at room temperature for 3 h. Then, the flask was heated at 60 °C for 1 h and the dispersion was centrifuged to separate the grinded peels of tangerine from the supernatant at 6000 rpm for 10 min. Finally, the extract solution obtained was stored in freezer until its use.

The magnetic core (magnetite) was synthesized using approximately 5.234 g of iron III nitrate nonahydrate ($Fe(NO_3)_{3.}\cdot 9H2O$), solubilized in 10 mL of distilled water in a 250 mL round bottom flask. Then, about 7 mL of the tangerine extract were added dropwise. The solution was placed into the drying oven at 80 °C for 6.5 h. The flask was then placed in an oil bath on a magnetic stirring plate and submitted to a flow of N_2 for 1 h at 25 °C to ensure an inert atmosphere therein. Later, the solution was heated at 180 °C for 3 h. After this procedure, the product obtained was washed with distilled water to neutral pH, by centrifugation at 600 rpm during 5 minutes. The resultant material was dried in oven overnight at 60 °C.

3.2.2 Coating process

The coating process of the magnetic nanoparticles is illustrated in Figure 4.

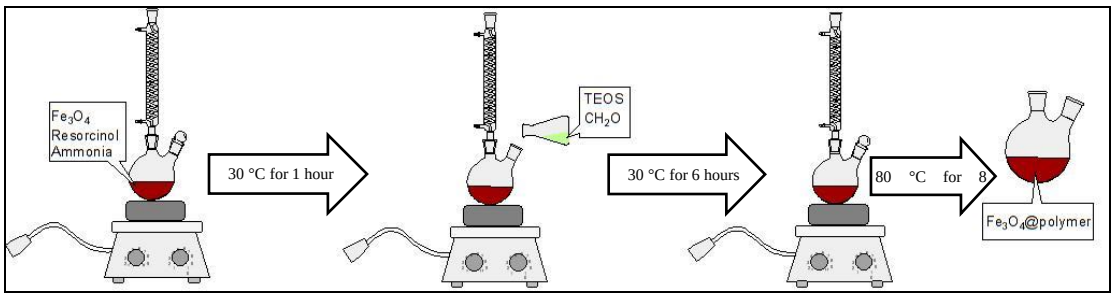

Figure 4 - Coating process of the magnetic nanoparticles.

For the coating, a mass of approximately 0.25 g of nanoparticles was measured and placed into a 250 mL erlenmeyer flask, containing 150 mL of absolute ethanol and 50 mL of distilled water. The solution was placed in an ultrasonic bath, Ultrasons-H, P-

Selecta (Figure VI - Annex A), at room temperature, until all the magnetite particles were dispersed in the medium [52].

The dispersion was transferred to a 500 mL round bottom flask, which contained 0.100 g of Resorcinol and 1.4 mL of a 25% ammonia solution. The flask was placed in an oil bath and stirred with a magnetic stirrer at 30 °C for 1 h. Subsequently, 210 μL of TEOS and 150 μL of formaldehyde (37-40%) were added dropwise and stirred for 6 h at 30 °C. After that time, the temperature was raised to 80 °C and the flask remained at this temperature for 8 h [52]. The resulting polymer-coated nanoparticles was washed with distilled water until neutral pH, using a centrifuge (6000 rpm for 5 min) and finally with absolute ethanol. The resultant material was then dried overnight and subsequently weighted and stored in vial.

At the second step of the coating process, the polymer-coated nanoparticles was carbonized under a N_2 atmosphere in a vertical tubular furnace (ROS 50/250/12, Thermoconcept, Figure VII- Annex A). The gas phase thermal treatment under a N_2 flow (100 $Ncm^3.min^{-1}$) was conducted at 120 °C and 400 °C during 1 h at each temperature and then at 600 °C for 4 h using heating rates, in each case, of 2 $°C.min^{-1}$. The resultant carbon-coated MNPs were denoted as $Fe_3O_4@SiO_2.C$ [45,52] .

3.2.3 Silica etching

$Fe_3O_4@SiO_2.C$ nanoparticles were etched under stirring with a sodium hydroxide solution 10 M. 10 mg of nanoparticles was added to 1 mL of the NaOH solution. The Erlenmeyer, containing the suspension, was placed on a magnetic stirrer and left under vigorous magnetic stirring for 16 h [45,52]. The resulting material was washed with distilled water to neutral pH using a centrifuge (6000 rpm for 5 min) and then washed with absolute ethanol. The material was dried overnight at 60 ºC in oven, resulting in the yolk carbon shell magnetic nanoparticles (YCSMNP). After drying the sample was weighted and stored in vial.

3.2.4 Chemical treatment

The colloidal stabilization of the YCSMNPs was increased by a chemical treatment with acid, incorporating carboxylic and hydroxyl groups, without compromising the magnetic core. The YCSMNPs were suspended in a HNO_3 solution (1 M) with a ratio of 5 mg of YCSMNPs per 1 mL of HNO_3 solution. The flask containing that suspension was placed in a oil bath at 65 °C with magnetic stirring for 3 h [45,52]. Subsequently, the resulting material was washed with distilled water until neutral pH using a centrifuge (6000 rpm for 5 min) and then washed with absolute ethanol. The material was further dried at 60 ºC in oven overnight. After drying it was weighted and stored in vial.

3.2.5 Funcionalization with pluronic F-127

After performing the chemical treatment, the resulting material was functionalized with Pluronic F-127 (PF127). For this purpose, a mass of approximately 40 mg of the chemical treated YCSMNP was measured and dispersed in 20 mL of distilled water with ultrasounds. Then, 800 mg of PF127 was added and magnetically stirred for 5 h at room temperature [52]. The resulting solution was washed by centrifugation (13 000 rpm, 20 min) with distilled water to remove unbounded copolymer and the resulting material was dried in oven at 60 °C for 8 h, resulting in the functionalized sample FYCSMNP.

3.3 Characterization

The magnetic core was characterized by X-ray diffraction (XRD) in order to perform phase identification and to determine the crystalline structure and the total core size. XRD analysis was performed in a PANalytical X'Pert MPD equipped with a X'Celerator detector and a secondary monochromator (Cu Kα λ= 0.154 nm; data recorded at a 0.017° step size). The composition of magnetite present was identified using HighScore software and Crystallography Open Database. Crystallite sizes were determined by the Halder–Wagner method [82]. The effects of the functionalization were analyzed using the spectral analysis in the Fourier transform infrared spectrometer (FT - IR), in a PerkinElmer equipment.

3.4 Drug loading and release

Phosphate buffer solutions (PBS) with different pH were used for the drug loading and release tests. These solutions were prepared as following: a) PBS pH 4.5: 3.40 g of dihydrogen potassium phosphate was diluted in 0.5 L of distilled water; b) PBS pH 6.0: 24.6 mL of $Na_2HPO_4 \cdot 12H_2O$ (0.2 M) solution was mixed with 175.4 mL of $NaH_2PO_4 \cdot H_2O$ (0.2 M) solution; c) PBS pH 7.4: 95 mL of of $NaH_2PO_4 \cdot H_2O$ (0.2 M) was mixed with 405 mL of $Na_2HPO_4 \cdot 12H_2O$ (0.2 M) solution.

3.4.1 Drug loading

For the DOX loading, a solution of 1000 $\mu g.mL^{-1}$ was used. To produce this solution, a mass of 25 mg of DOX was weighted and dissolved in 5 mL of distilled water. 4 mL of this solution was further diluted in 20 mL of PBS (pH 7.4) solution. After that, 20 mg of the FYCSMNP was measured and dissolved in 20 mL of PB (7.4) solution with the aid of ultrasound until the solutions were homogeneous.

For the OME loading, a solution of 250 $\mu g.mL^{-1}$ was used. To produce this solution a mass of 12.5 mg of the drug was measured and dissolved in 50 mL of distilled water. 12.5 mg of FYCSMNP were then added to the solution.

The drug loading was conducted by mixing the solution of the FYCSMNP and the drug solution under agitation in a IKA® KS 130 basic orbital shaker (Figure VIII -Annex A), for 48 h, at room temperature [7]. Then, the resulting suspension was centrifuged (6000 rpm for 5 min) and the bottom body containing the drug loaded FYCSMNP lyophilized and stored in a freezer until its use. The supernatant was taken to analyze by the T70 UV-VIS spectrophotometer, PG Instruments Ltd. (Figure IX -Annex A) for determination of DLC and DLE, at 480 nm for the DOX and 300 nm for the OME, as follow:

$$DLC = \frac{C_{DRUG-FYCSMNPs}}{C_{FYCSMNPs}}$$

$$DLE(\%) = \frac{C_{0DRUG} - C_{fDRUG}}{C_{0DRUG}} * 100$$

Where, $C_{DRUG\text{-}FYCSMNPs}$ is the concentration of drug (DOX and OME) loaded in the FYCSMNPs ($\mu g.mg^{-1}$), $C_{FYCSMNPs}$ is the concentration of FYCSMNPs, C_{0Drug} is the initial concentration of the drugs solution before the loading ($\mu g.mL^{-1}$), $C_{f\ DRUG}$ is the final concentration of the drugs measured in supernatant after the loading ($\mu g.mL^{-1}$). The concentration of drug loaded in the FYCSMNPs is measured by subtracting the concentration of the drug in the supernatant from the initial concentration of the drug solution. These concentrations were calculated using the calibration curves shown in Figure 5.

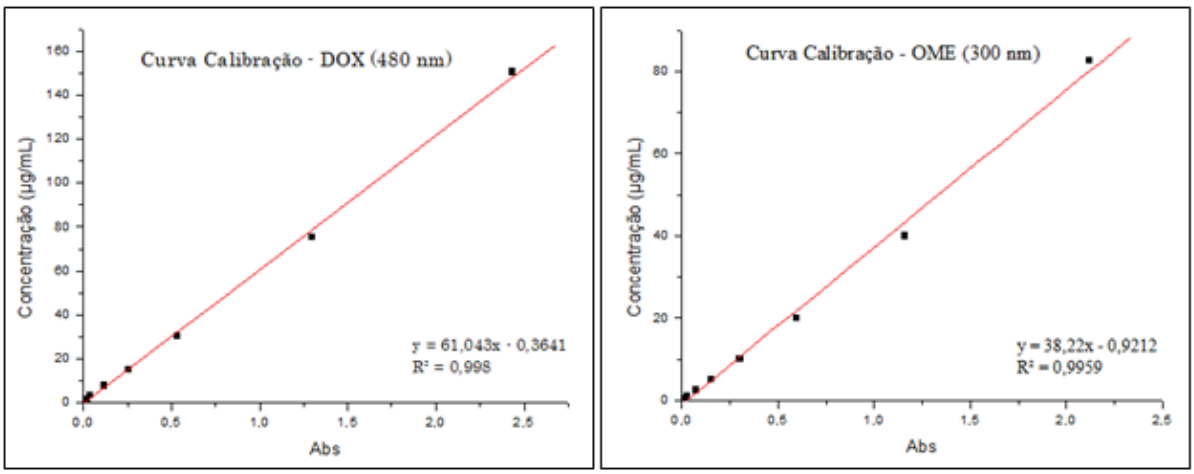

Figure 5- Calibration curves for determination of DOX and OME concentrations by UV-Vis spectrophotometry.

3.4.2 Drug release

The release tests were carried out in duplicate for different solutions of PBS at physiological (pH 7.4) and acidic pH levels (pH 4.5 and 6.0). To perform the release of the drug, masses between 1 mg and 2 mg of nanoparticles lyophilized with the drug were measured and then added to 10 mL of buffer solutions at different pHs. The solutions were homogenized with ultrasonic bath.

The flasks were placed in a orbital shaker and maintained in oven at 37 °C (human body temperature) under constant stirring during the release test. The mixture was centrifuged to separate the FYCSMNP of the supernatant at the following selected times: 0.5, 1, 2, 4, 6, 24 and 48 h. After each centrifugation, the FYCSMNPs returned to the flask, where 10 mL of the same solution were added and the flasks returned to the orbital shaker and to the oven, to continue the release of the drug. The supernatant separated in the centrifugation was measured by UV-Vis spectrophotometry at 480 nm to identify the concentration of drug that was released in each solution at each time, using the calibration curves shown in Figure 5.

The whole process of analysis of the drug release tests was also repeated with the CCYSMNP loaded with OME. But the supernatant was measured by UV-Vis spectrophotometry at 300 nm to quantify the concentration of the OME that was released in each solution, using the calibration shown in the Figure 5.

Chapter 4: Results and Discussion

4 Results and Discussion

4.1 Synthesis of iron oxide nanoparticles

The particles produced by SCS with citric acid and with the tangerine extract, by the procedure described in the previous chapter, are shown in Figure 6. It is noted that the particles produced with citric acid are magnetic, in opposition to the particles produced with the extract.

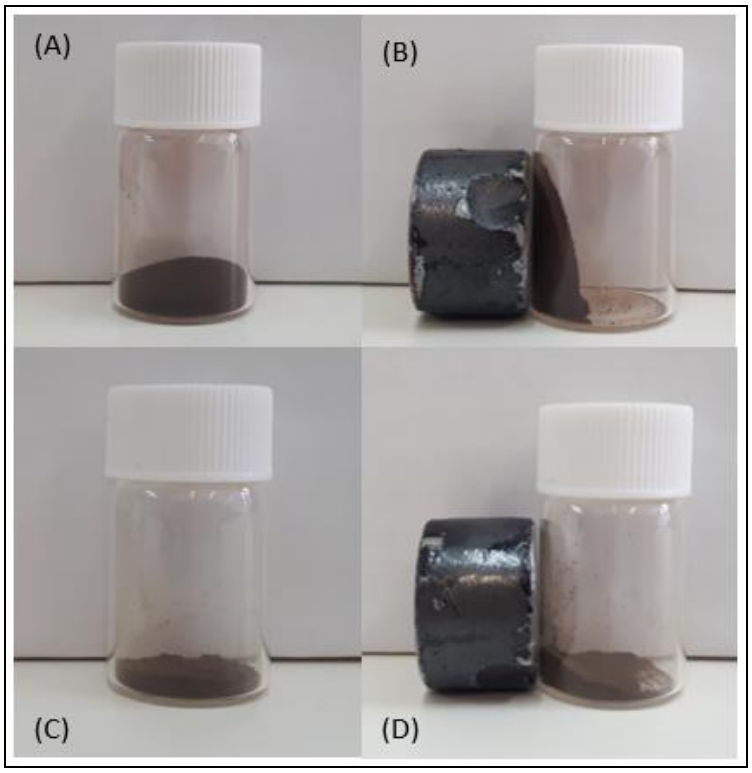

Figure 6 – Nanoparticles produced with SCS. (A) Nanoparticles produced with citric acid without magnetic influence. (B) Nanoparticles produced with citric acid in the presence of a magnet. (C) Nanoparticles produced with tangerine extract without magnetic influence. (D) Nanoparticles produced with tangerine extract in the presence of a magnet.

X-ray diffraction (XRD) was used to characterize the crystallography of the obtained MNPs. The XRD spectrum is presented in Figure 7 and shows characteristic peaks at 30.32º (220), 35.70º (311), 43.35º (400), 53.69º (422), 57.18º (511) and 62.82º (440), corresponding to magnetite nanoparticles. Peaks were referenced with standard peaks in the Joint Committee on Powder diffraction standard (JCPDS) file (PDF N° 65– 3107) [83,84]. Therefore, the

investigation of phase by XRD confirms that the crystal structure of the core synthesized with the citric acid corresponds to that of magnetite. The average particle size calculated by the Halder–Wagner method is around 19.3 nm.

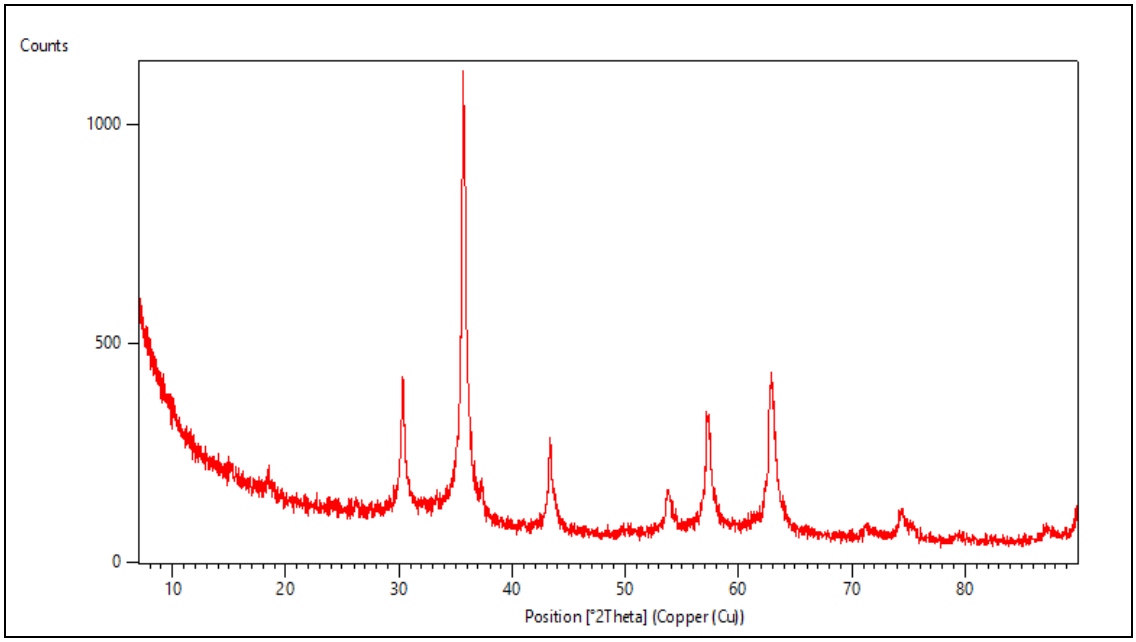

Figure 7- XRD patterns of the magnetic cores synthesized with citric acid.

The XRD spectra of the nanoparticles produced with the tangerine extract, in Figure 8, shows characteristic peaks at 18.47°, 23.20°, 29.01º, 34.50º, 42.86º, 45.38°, 48.29º and 57.39º,which does not correspond to magnetite nanoparticles, as referenced with standard peaks in the Joint Committee on Powder diffraction standard (JCPDS) file (PDF N° 65-3107) [83,84].

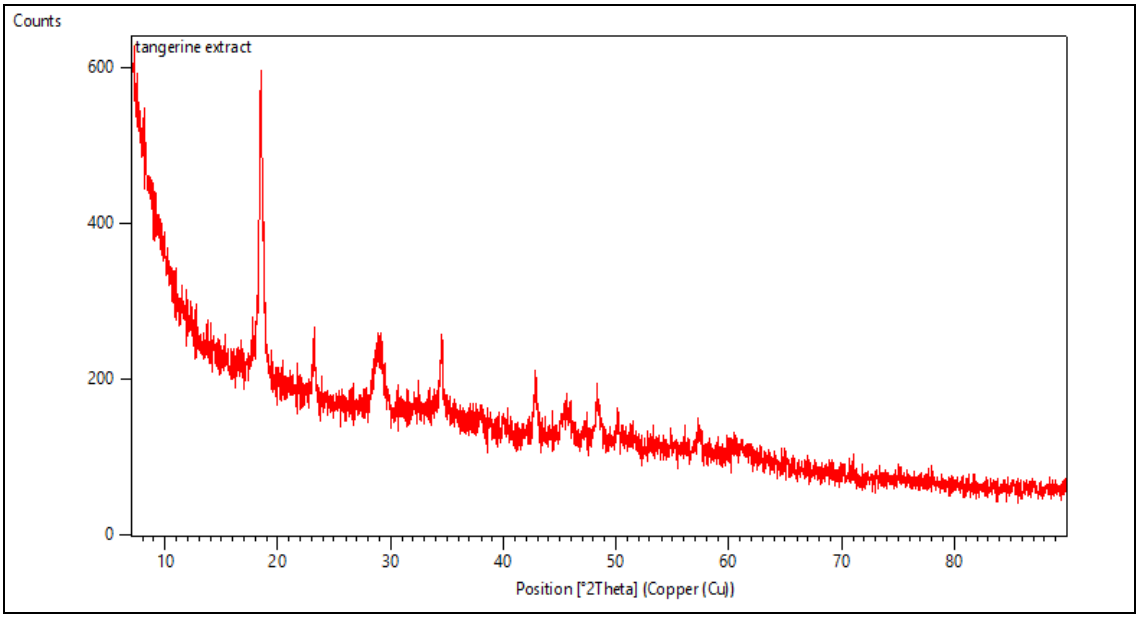

Figure 8 - XRD patterns of the magnetic cores synthesized with the tangerine extract.

Taking into consideration the non-magnetic behavior of the nanoparticles synthesized with the tangerine extracts (as shown in Figure 6), not corresponding to the crystal structure of magnetite nanoparticles, it was decided to not continue the rest of the methodology with the particles produced with the tangerine extracts.

4.2 The effects of the functionalization

The spectral analysis done by Fourier transform infrared spectrometry (FT-IR) was performed to study the effects of the functionalization. The comparison of the spectra of the nanocomposites before and after functionalization is shown in Figure 9. The presence of magnetite is noticed in the absorption bands of 564 cm^{-1}, 1635 cm^{-1} and 3436 cm^{-1}. The first band corresponds to the vibration of the Fe–O bond and the latter two can be attributed to the bending and stretching vibrations of the surface –OH groups present in Fe_3O_4 [85,86]. The absorption bands at 1384 cm^{-1} , 1458 cm^{-1}, 1632 cm^{-1}, 2917 cm^{-1} and 3436 cm^{-1} represent the C-O, O-H, C=O, C-H and O-H bonds respectively, which indicate that there are carboxylic acid groups in the samples [7].

In the functionalized sample, the increase in the intensity of the absorption bands at 1384 cm^{-1} and 1632 cm^{-1} represents the increase in the C-O and C=O bonds of the carboxylic

acid groups [87]. This indicates the increase of the carboxyl, which are responsible for making the nanocomposites more acidic. The presence of these groups in nanocomposites can improve the colloidal stability and monodispersibility in aqueous solutions [7].

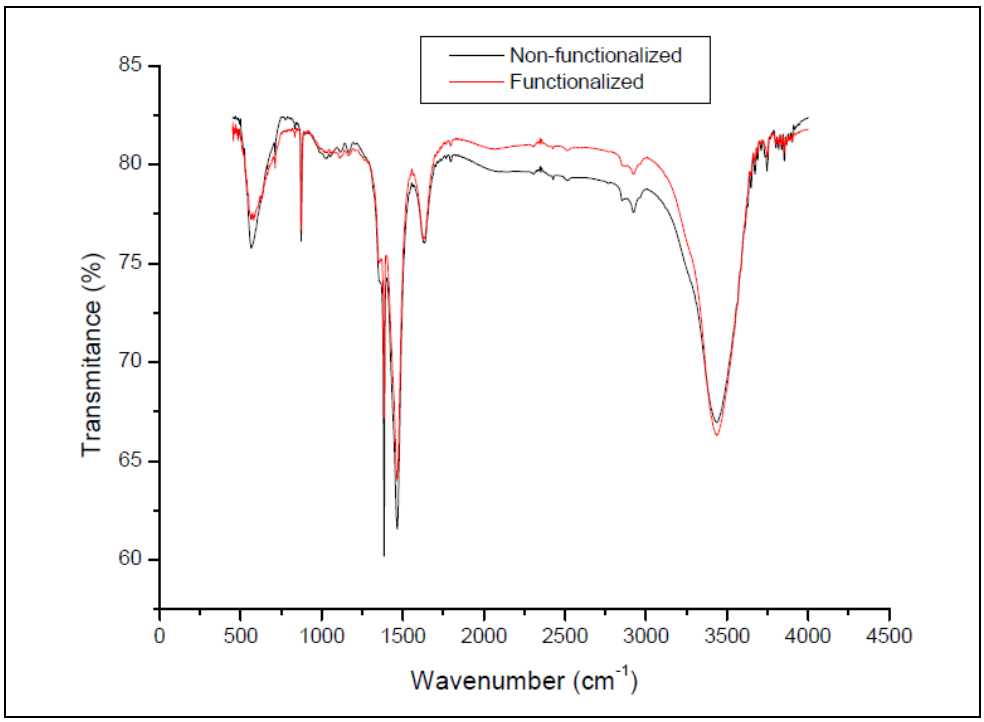

Figure 9 - FT-IR spectra of the functionalized and non-functionalized YCSMNP.

4.3 Yield of the nanomaterials obtained

The yield of the production of the nanomaterials is shown in Table 1. For the synthesis, according to the stoichiometry shown in equation 1, for each mol of $Fe(NO_3)_3$ considered, 0.85 mol of citric acid is needed and 0.33 mol of Fe_3O_4 is produced. In this work, using 0.01296 mol of $Fe(NO_3)_3$ and 0.01103 mol of citric acid, 0.00384 mol of Fe_3O_4 was obtained, corresponding to an yield of reaction of 89.79%,.

The yield in the first step of the coating process is 24.77%, producing an average of 0.1757 g of material in each process. In the second step of the coating, a loss of 35% of the mass in the carbonization was observed. In the following steps of the process, an additional loss of mass of 5.60% was observed in the etching process and 45% in the acid treatment. In the functionalization with Pluronic, an increase of 6% was observed in the mass of the nanostructures.

Table 1- Yield of the nanomaterials obtained.

		Mass (g)	***Total mass(g)***	***Final mass (g)***	***Yield (%)***
Synthesis	$Fe(NO_3)_3$	5.234	7.5538	0.8889	89.79
	Citric Acid	2.3198			
	MNPs	0.25	0.7094	0.1757	24.77
Coating	Formaldehyde	0.1635			
	TEOS	0.1959			
	Resorcinol	0.1			
Carbonization	MNPs	3.33	3.33	2.2176	65.00
Etching	MNPs	0.1		0.094	94.40
HNO_3	MNPs	0.9053		0.4921	54.36
Funcionalization	MNPs	0.04		0.0426	106

4.4 Capacity and efficiency of drug loading

The DLC ($\mu g.\mu g^{-1}$) and DLE (%) were studied for solutions of two drugs, DOX and OME, with the functionalized CCYSMNPs. For the studies with DOX a solution media of PBS pH 7.4 was used and for the studies with OME, distilled water was used. The results are shown in Table 2.

Table 2 - Results of drug loading for DOX and OME.

Drug	**DLC ($\mu g.\mu g^{-1}$)**	**DLE (%)**
Doxorubicine	0.936	93.6
Omeprazole	0.335	33.5

As observed, both DLC and DLE was higher when DOX was considered (0.936 $\mu g.\mu g^{-1}$ and 93.6% respectively), than those values obtained when OME was loaded (0.335 $\mu g.\mu g^{-1}$ and 33.5%). Comparing the results obtained with DOX with previous works, it can be noticed that the obtained values are very similar, 0.914 $\mu g \cdot \mu g^{-1}$ and 91.4% [7] for DLC and DLE, respectively for the nanomaterial with magnetic core (magnetite) synthetized by co-precipitation and with loading process of 24 h.

The loading results of DOX can be compared with an others drug delivery system. A polypeptide-based nanoparticles system have a DLE of around 97% [88]. In other study,

magnetic NCs consist on hybrid nanostructure, which were obtained by an oil-in-water microemulsion, shows a DLE up to 24.39% [89].

4.5 The effect of pH on drug release

The analysis of the pH effect on the drug release is very important due to the difference between the pH of the normal tissues (pH 7.4) and the extracellular environment of the tumor (pH < 6.5). A pH-sensitive drug delivery system is usually used to improve the drug release in tumor tissues due to the low pH value of tumor tissues [90]. If more drug is released in the more acidic environment, the lower will be the side effects and damage to the healthy cells. In these release tests higher drug release values in acidic medium were expected for both of the drugs studied.

The cumulative drug release (%) of the amount of DOX retained in the nanocomposites are 39.33%, 29.05% and 7.10% in PBS solutions with pH 4.5, pH 6.0 and pH 7.4, respectively, Figure 10a. These results can be expressed in cumulative concentrations of 51.70 μg.mL^{-1}, 38.64 μg.mL^{-1} and 7.94 μg.mL^{-1}, represent in weight DOX quantities of 516.97 μg, 386.42 μg and 79.37 μg in PBS solutions with pH 4.5, pH 6.0 and pH 7.4, respectively. The drug release over time is represented in Figure 10b. As expected, for DOX, the largest amount of drug released was obtained in the acid medium, which indicates that the FYCSMNPs works as a DOX drug delivery system.

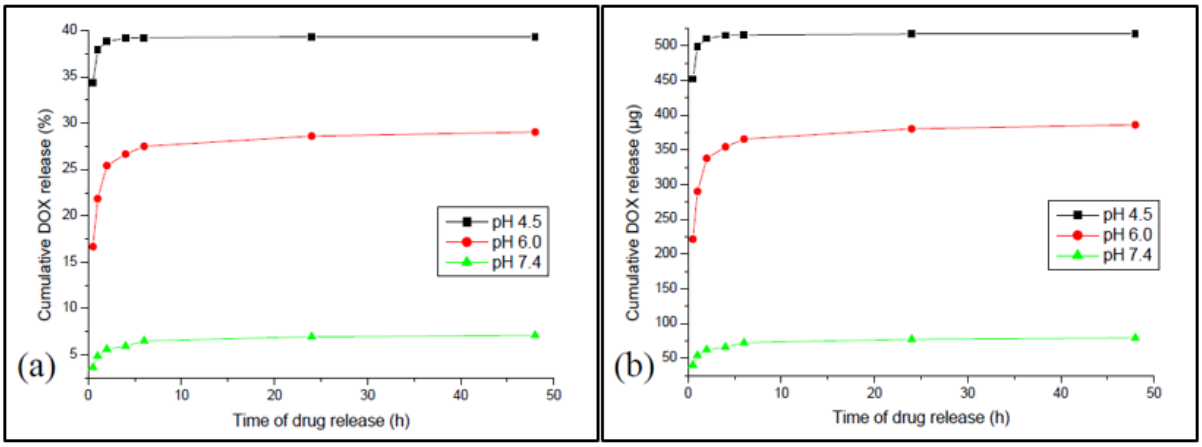

Figure 10 - (a) Cumulative DOX release (%). (b) Cumulative DOX release (μg).

Analyzing the results obtained for DOX release, it can be concluded that they are slightly higher than those obtained in previous works (21%) which the magnetic core (magnetite) of the nanomaterial synthetized by co - precipitation [7], having a better delivery in the more acid medium (pH < 6.5).

A polypeptide-based nanoparticles system also have a better drug release (60%) at the most acid medium (pH 5.5) tested when compared to the drug release (22%) at pH 7.4, so the health tissue medium, [88]. Drug release of 20% and 80% at pH 7.4 and pH 5.5 have been obtained with magnetic NCs is a hybrid nanostructure were obtained by an oil-in-water microemulsion, respectively [89] .

The cumulative drug release (%) of the amount of OME retained in the nanocomposites are 35.01%, 49.53% and 49.21% in PBS solutions with pH 4.5, pH 6.0 and pH 7.4, respectively, Figure 11a. These results can be expressed in cumulative concentrations of 12.50 μg.L^{1}, 19.21 μg.mL^{-1} and 19.44 μg.mL^{-1}, which represent in weight of OME the quantities of 125.01 μg, 192.08 μg and 194.37 μg in PBS solutions with pH 4.5, pH 6.0 and pH 7.4, respectively. The drug release over time is represented in Figure 11b.

In the studies carried out with OME, the results were not as expected, since as OME is a drug used in the treatment of active duodenal ulcers, active benign gastric ulcers, gastro-esophageal reflux disease, a much greater drug release in the acidic pH was desired.

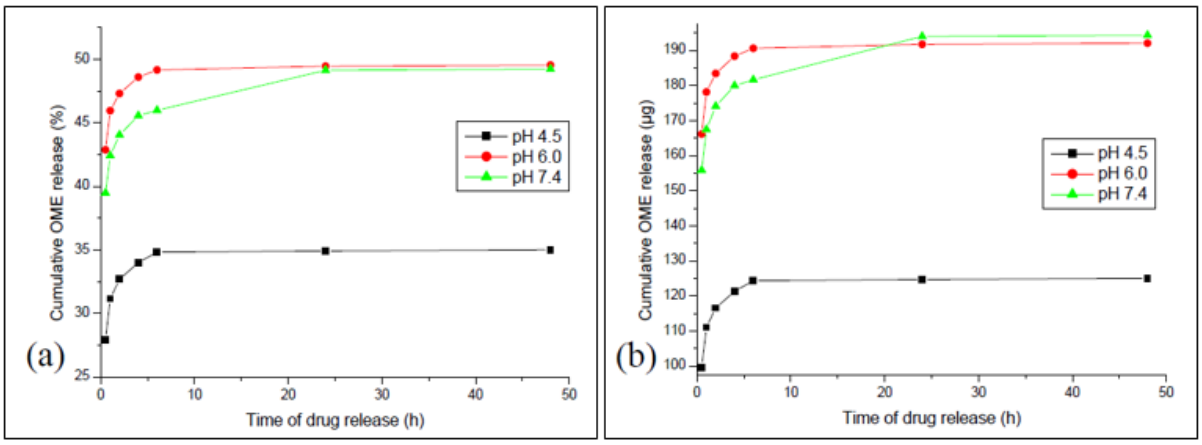

Figure 11- (a) Cumulative OME release (%). (b) Cumulative OME release (μg).

The drug release has shown to have a dependence with the pH of the targeting cells, for the DOX, the medium with pH 4.5 and for the OME, pH 6.0. Therefore, pH controlled drug release would be a viable application to the synthesized material. For this application,

the FYCSMNPs would be conducted to the target with a magnetic field and the pH of the environment would act on the release of the drug. The disadvantage is that a large part of the drug loaded in the particles was not released.

In conclusion, this research demonstrates that the FYCSMNPs developed have an outstanding ability as drug nanocarriers, in the case of the Doxorubicine with great ability to load high content of the drug.

Chapter 5: Conclusions and Future Research

5. Conclusions and Future Research

5.1 Conclusions

Based on the premise of optimizing yolk-shell magnetic nanocomposites for applications in biomedicine, this thesis was conducted aiming to obtain higher amount of drug release in a more acidic medium, mimicking the medium of tumor tissues. Thus, considering all the adjustments made during the synthesis, coating, functionalization and loading and release of the drug, the final result obtained shows a quantity of released DOX much higher in the acid medium when compared to the equivalent pH in normal cells. But, in the case of OME the higher amount of drug was releases at pH 6.0.

A disadvantage of the developed system was the high amount of both drugs retained in the material, still requiring furher optimization to improve the drug exploitation and to obtain better yield of release. Another parameter that needs optimization is the first step of the coating process, to try to reduce the amount of mass loss in this step of the methodology.

5.2 Future Research

Looking forward to develop a better drug delivery system, some details of the process need to be polished. The coating process needs to be study, to achieve a lower value of mass loss. Relating to loading of the drugs, the loading of OME needs to be improved, so that a higher quantity of the drug can be loaded into the FYCSMNP. To try to solve this problem, maybe instead of 48 h, the loading process could be longer. Also, the drug release needs to be improved for both drug, so that fewer amount of them are maintained in the nanocomposites.

Chapter 6: References

References

1. Ramanujan, R. V. Magnetic particles for biomedical applications. *Biomed. Mat.* 477–491 (2009).
2. Huang, M. *et al.* Magnetic iron nanoparticles prepared by solution combustion synthesis and hydrogen reduction. *Chem. Phys. Lett.* **657**, 33–38 (2016).
3. Ianoş, R., Tăculescu, A., Păcurariu, C. & Lazău, I. Solution combustion synthesis and characterization of magnetite, Fe_3O_4, nanopowders. *J. Am. Ceram. Soc.* **95**, 2236–2240 (2012).
4. Deganello, F. & Tyagi, A. K. Solution combustion synthesis, energy and environment: Best parameters for better materials. *Prog. Cryst. Growth Charact. Mater.* **64**, 23–61 (2018).
5. Makarov, V. V *et al.* 'Green' nanotechnologies: synthesis of metal nanoparticles using plants. *Acta Naturae* **6**, 35–44 (2014).
6. Singh, A. K. & Srivastava, O. N. One-step green synthesis of gold nanoparticles using black cardamom and effect of pH on its synthesis. *Nanoscale Res. Lett.* **10**, 353 (2015).
7. Paula, R. De. Development and functionalization of magnetic nanocomposites for cancer treatment. Master Thesis, IPB. (2017).
8. Francisquini, E., Schoenmaker, J. & Souza, J. A. Nanopartículas magnéticas e suas aplicações. *Quím. Supramolec. e Nanotec.* (2014).
9. Camilo, R. L. 'Síntese e caracterização de nanopartículas magnéticas de ferrita de cobalto recobertas por 3-aminopropiltrietoxissilano para uso como material híbrido em nanotecnologia'. Doctorate Thesis, USP. (2006).
10. Maboudi, S. A., Shojaosadati, S. A. & Arpanaei, A. Synthesis and characterization of multilayered nanobiohybrid magnetic particles for biomedical applications. *Mater. Des.* **115**, 317–324 (2017).
11. Gangwar, A. *et al.* Fe3C nanoparticles for magnetic hyperthermia application. *J. Magn. Magn. Mater.* **481**, 251–256 (2019).
12. Orhan, H. *et al.* Bacteria killer enzyme attached magnetic nanoparticles. *Mater. Sci. Eng. C* **94**, 558–564 (2019).
13. Liu, J., *et al* . One-pot synthesis of Ag– Fe_3O_4 nanocomposites in the absence of additional reductant and its potent antibacterial properties. *J. Mater. Chem.* **22**, 13891 (2012).
14. Abbas, M. *et al.* Highly stable- silica encapsulating magnetite nanoparticles (Fe_3O_4/SiO_2) synthesized using single surfactantless- polyol process. *Ceram. Int.* **40**, 1379–1385 (2014).
15. Brito, E. L. *et al.* Superparamagnetic magnetite/IPEC particles. *Colloids Surfaces A Physicochem. Eng. Asp.* **560**, 376–383 (2019).
16. Lu, A.-H., Salabas, E. L. & Schüth, F. Magnetic Nanoparticles: Synthesis, Protection, Functionalization, and Application. *Angew. Chemie Int. Ed.* **46**, 1222–1244 (2007).

17. Chen, Z. *et al.* Synthesis, functionalization, and nanomedical applications of functional magnetic nanoparticles. *Chinese Chem. Lett.* **29**, 1601–1608 (2018).

18. Ye, W., *et al* . Recyclable, non-leaching antimicrobial magnetic nanoparticles. *Chinese Chem. Lett.* (2019)

19. Bandeira, A. C. *et al.* Is it possible to track intracellular chitosan nanoparticles using magnetic nanoparticles as contrast agent? *Bioorg. Med. Chem.* **27**, 2637–2643 (2019).

20. Issa, B. *et al.* Magnetic nanoparticles: surface effects and properties related to biomedicine applications. *Int. J. Mol. Sci.* **14**, 21266–21305 (2013).

21. Favela-Camacho, S. E., *et al* . How to decrease the agglomeration of magnetite nanoparticles and increase their stability using surface properties. *Colloids Surfaces A Physicochem. Eng. Asp.* **574**, 29–35 (2019).

22. Yuri A. Barnakov, *et al* . Manipulation of the magnetic properties of magnetite−silica nanocomposite materials by controlled stober synthesis. (2005)

23. Ianoş, R. *et al.* Combustion synthesis of iron oxide/carbon nanocomposites, efficient adsorbents for anionic and cationic dyes removal from wastewaters. *J. Alloys Compd.* **741**, 1235–1246 (2018).

24. Cornell, R. M. & Schwertmann, U. The iron oxides : structure, properties, reactions, occurrences, and uses. *John Wiley & Sons.* (2003).

25. Shylesh, S., *et al*. Magnetically separable nanocatalysts: bridges between homogeneous and heterogeneous catalysis. *Angew. Chemie Int. Ed.* **49**, 3428–3459 (2010).

26. Wen, X. *et al.* Multifunctional magnetic branched polyethylenimine nanogels with in-situ generated Fe_3O_4 and their applications as dye adsorbent and catalyst support. *J. Mater. Sci.* **51**, 3170–3181 (2016).

27. Meng, Y. *et al.* Prediction on morphologies and phase equilibrium diagram of iron oxides nanoparticles. *Appl. Surf. Sci.* **480**, 478–486 (2019).

28. Simonsen, G., *et al*. Potential applications of magnetic nanoparticles within separation in the petroleum industry. *J. Pet. Sci. Eng.* **165**, 488–495 (2018).

29. Behrens, S. & Appel, I. Magnetic nanocomposites. *Curr. Opin. Biotechnol.* **39**, 89–96 (2016).

30. Savadkoohi, M., *et al*. Using silicon nanoparticles to modify the surface of graphene nanosheets. *Mater. Sci. Semicond. Process.* **75**, 75–83 (2018).

31. Nasiri, P., *et al* . Synthesis of Au/Si nanocomposite using laser ablation method. *Opt. Laser Technol.* **113**, 217–224 (2019).

32. Mehrani, A., *et al* . Properties of Au/ZnO nanocomposite prepared by laser irradiation of the mixture of individual colloids. *J. Clust. Sci.* **26**, 1743–1754 (2015).

33. Liu, J., *et al* . Magnetic nanocomposites with mesoporous structures: synthesis and applications. *Small* **7**, 425–443 (2011).

34. Liu, W. *et al.* One-pot synthesis of yolk–shell mesoporous carbon spheres with high magnetisation. *J. Mater. Chem. A* **2**, 9600–9606 (2014).

35. Faraji, M., *et al*. Magnetic nanoparticles: synthesis, stabilization, functionalization,

characterization, and applications. *J. Iran. Chem. Soc.* **7**, 1–37 (2010).

36. Asgari, S., Saberi, A. H., McClements, D. J. & Lin, M. Microemulsions as nanoreactors for synthesis of biopolymer nanoparticles. *Trends Food Sci. Technol.* **86**, 118–130 (2019).

37. Nadimpalli, N. K. V., Bandyopadhyaya, R. & Runkana, V. Thermodynamic analysis of hydrothermal synthesis of nanoparticles. *Fluid Phase Equilib.* **456**, 33–45 (2018).

38. Mahajan, D., Papish, E. T. & Pandya, K. Sonolysis induced decomposition of metal carbonyls: kinetics and product characterization. *Ultrason. Sonochem.* **11**, 385–392 (2004).

39. Aisida, S. O. *et al.* Biosynthesis of silver nanoparticles using bitter leave (Veronica amygdalina) for antibacterial activities. *Surfaces and Interfaces* **17**, 100359 (2019).

40. Zhang, H. *et al.* Biosynthesis of selenium nanoparticles mediated by fungus Mariannaea sp. HJ and their characterization. *Colloids Surfaces A Physicochem. Eng. Asp.* **571**, 9–16 (2019).

41. Li, F., Ran, J., Jaroniec, M. & Qiao, S. Z. Solution combustion synthesis of metal oxide nanomaterials for energy storage and conversion. *Nanoscale* **7**, 17590–17610 (2015).

42. Selvan, R. K., Augustin, C., Berchmans, L. J. & Saraswathi, R. Combustion synthesis of $CuFe_2O_4$. *Mater. Res. Bull.* **38**, 41–54 (2003).

43. Harshiny, M., Iswarya, C. N. & Matheswaran, M. Biogenic synthesis of iron nanoparticles using Amaranthus dubius leaf extract as a reducing agent. *Powder Technol.* **286**, 744–749 (2015).

44. Smuleac, V., *et al*. Green synthesis of Fe and Fe/Pd bimetallic nanoparticles in membranes for reductive degradation of chlorinated organics. *J. Memb. Sci.* **379**, 131–137 (2011).

45. Oliveira, J. R. P. *et al.* Carbon-based magnetic nanocarrier for controlled drug release : a green synthesis approach. *J. Carbon Res.* **5**, (2018).

46. Parveen, K., Banse, V. & Ledwani, L. Green synthesis of nanoparticles: their advantages and disadvantages. in *AIP Conference Proceedings* vol. 1724 020048 (AIP Publishing LLC, 2016).

47. Gingasu, D. *et al.* Green synthesis methods of $CoFe_2O_4$ and Ag-$CoFe_2O_4$ nanoparticles using hibiscus extracts and their antimicrobial potential. *J. Nanomater.* **2016**, 1–12 (2016).

48. Priebe, M. & Fromm, K. M. Nanorattles or Yolk-shell nanoparticles-what are they, how are they made, and what are they good for? *Chem. - A Eur. J.* **21**, 3854–3874 (2015).

49. Dayana, I. *et al.* The effect of tetraethyl orthosilicate (TEOS) additions as silica precursors on the magnetite nano-particles (Fe_3O_4) properties for the application of ferro-lubricant. *J. Mol. Liq.* **294**, 111557 (2019).

50. Barberena-Fernández, A. M., Blanco-Varela, M. T. & Carmona-Quiroga, P. M. Use of nanosilica- or nanolime-additioned TEOS to consolidate cementitious materials in heritage structures: Physical and mechanical properties of mortars. *Cem. Concr. Compos.* **95**, 271–276 (2019).

51. Fuertes, A. B., Valle-Vigón, P. & Sevilla, M. One-step synthesis of silica@resorcinol-formaldehyde spheres and their application for the fabrication of polymer and carbon capsules. *Chem. Commun.* **48**, 6124–6126 (2012).

52. Rodrigues, R. O. *et al.* Multifunctional graphene-based magnetic nanocarriers for combined hyperthermia and dual stimuli-responsive drug delivery. *Mater. Sci. Eng. C* **93**, 206–217 (2018).

53. Hayes, R., *et al* . Core–shell particles: Preparation, fundamentals and applications in high performance liquid chromatography. *J. Chromatogr. A* **1357**, 36–52 (2014).

54. Liu, J. *et al.* Yolk/shell nanoparticles: new platforms for nanoreactors, drug delivery and lithium-ion batteries. *Chem. Commun.* **47**, 12578 (2011).

55. Purbia, R. & Paria, S. Yolk/shell nanoparticles: classifications, synthesis, properties, and applications. *Nanoscale* **7**, 19789–19873 (2015).

56. Scott, J. H. J. & Majetich, S. A. Morphology, structure, and growth of nanoparticles produced in a carbon arc. *Phys. Rev. B* **52**, 12564–12571 (1995).

57. Charles, S. W. & Popplewell, J. Properties and applications of magnetic liquids. *Endeavour* **6**, 153–161 (1982).

58. Chenjie Xu, *et al.* Dopamine as a robust anchor to immobilize functional molecules on the iron oxide shell of magnetic nanoparticles. *Am. Chem. Soc.* **126**, 9938–9939 (2004).

59. Chenjie Xu, *et al.* Nitrilotriacetic acid-modified magnetic nanoparticles as a general agent to bind histidine-tagged proteins. *Am. Chem. Soc.* **126**, 3392–3393 (2004).

60. Narayan, R. Biomedical materials. *Biomed. Mater.* 1–566 (2009).

61. Sun, Y.-P., Li, X., Cao, J., Zhang, W. & Wang, H. P. Characterization of zero-valent iron nanoparticles. *Adv. Colloid Interface Sci.* **120**, 47–56 (2006).

62. C.-B. W. & Zhang*, W. Synthesizing nanoscale iron particles for rapid and complete dechlorination of TCE and PCBs. *Am. Chem. Soc.* **31**, 2154–2156 (1997).

63. Mues, B., *et al*. Towards optimized MRI contrast agents for implant engineering: clustering and immobilization effects of magnetic nanoparticles. *J. Magn. Magn. Mater.* **471**, 432–438 (2019).

64. Lin, Y.-L., *et al*. Renal perfusion assessment using magnetic nanoparticles with 7T dynamic susceptibility contrast MRI in rats. *J. Magn. Magn. Mater.* **475**, 76–82 (2019).

65. Arsalani, S. *et al.* Magnetic Fe_3O_4 nanoparticles coated by natural rubber latex as MRI contrast agent. *J. Magn. Magn. Mater.* **475**, 458–464 (2019).

66. Shirvan, A. R., Bashari, A. & Hemmatinejad, N. New insight into the fabrication of smart mucoadhesive buccal patches as a novel controlled-drug delivery system. *Eur. Polym. J.* (2019)

67. Chowdhury, S., *et al*. O. An overview of drug delivery vehicles for cancer treatment: nanocarriers and nanoparticles including photovoltaic nanoparticles. *J. Photochem. Photobiol. B Biol.* **164**, 151–159 (2016).

68. Pavitra, E. *et al.* Engineered nanoparticles for imaging and drug delivery in colorectal cancer. *Semin. Cancer Biol.* (2019).

69. Yallapu, M. M., *et al*. Therapeutic Applications of Curcumin Nanoformulations. *AAPS J.* **17**, 1341–1356 (2015).

70. Panyam, J. & Labhasetwar, V. Biodegradable nanoparticles for drug and gene delivery to cells and tissue. *Adv. Drug Deliv. Rev.* **55**, 329–347 (2003).

71. Redhead, H. M., Davis, S. S. & Illum, L. Drug delivery in poly(lactide-co-glycolide) nanoparticles surface modified with poloxamer 407 and poloxamine 908: in vitro characterisation and in vivo evaluation. *J. Control. Release* **70**, 353–363 (2001).

72. Singh, R. & Lillard, J. W. Nanoparticle-based targeted drug delivery. *Exp. Mol. Pathol.* **86**, 215–223 (2009).

73. Kumar, B., *et al*. Recent advances in nanoparticle-mediated drug delivery. *J. Drug Deliv. Sci. Technol.* **41**, 260–268 (2017).

74. Elansary, H. O. & Zin El-Abedin, T. K. Omeprazole alleviates water stress in peppermint and modulates the expression of menthol biosynthesis genes. *Plant Physiol. Biochem.* **139**, 578–586 (2019).

75. Zhu, K. *et al.* Repurposing of omeprazole for oligodendrocyte differentiation and remyelination. *Brain Res.* **1710**, 33–42 (2019).

76. Lin, M.-Z. *et al.* Antityrosinase mechanism of omeprazole and its application on the preservation of fresh-cut Fuji apple. *Int. J. Biol. Macromol.* **117**, 538–545 (2018).

77. Ronchi, F. *et al.* Development and evaluation of an omeprazole-based delayed-release liquid oral dosage form. *Int. J. Pharm.* **567**, 118416 (2019).

78. Albanez, R., Nitz, M. & Taranto, O. P. Enteric coating process of diclofenac sodium pellets in a fluid bed coater with a wurster insert: Influence of process variables on coating performance and release profile. *Adv. Powder Technol.* **24**, 659–666 (2013).

79. Singal, P. K. & Iliskovic, N. Doxorubicin-induced cardiomyopathy. *N. Engl. J. Med.* **339**, 900–905 (1998).

80. Arcamone, F. Doxorubicin : anticancer antibiotics. (Academic Press, 1981).

81. Kataoka, K. *et al.* Doxorubicin-loaded poly(ethylene glycol)–poly(β-benzyl-l-aspartate) copolymer micelles: their pharmaceutical characteristics and biological significance. *J. Control. Release* **64**, 143–153 (2000).

82. Izumi, F. & Ikeda, T. Implementation of the Williamson – Hall and Halder – Wagner Methods into RIETAN-FP. *Adv. Ceram. Res. Cent. Annu. Rep.* **3**, 33–38 (2014).

83. Nnadozie, E. C. & Ajibade, P. A. Green synthesis and characterization of magnetite (Fe_3O_4) nanoparticles using Chromolaena odorata root extract for smart nanocomposite. *Mater. Lett.* **263**, (2020).

84. Shahid, M. K. & Choi, Y. Characterization and application of magnetite Particles, synthesized by reverse coprecipitation method in open air from mill scale. *J. Magn. Magn. Mater.* **495**, (2020).

85. Bagavathi, M., Ramar, A. & Saraswathi, R. Fe_3O_4–carbon black nanocomposite as a highly efficient counter electrode material for dye-sensitized solar cell. *Ceram. Int.* **42**, 13190–13198 (2016).

86. de Mendonça, E. S. D. T. *et al.* Effects of silica coating on the magnetic properties of magnetite nanoparticles. *Surfaces and Interfaces* **14**, 34–43 (2019).

87. Wang, H., *et al*. Carboxyl and negative charge-functionalized superparamagnetic nanochains with amorphous carbon shell and magnetic core: Synthesis and their application in removal of heavy metal ions. *Nanoscale* **3**, 4600–4603 (2011).

88. Lv, S. *et al.* Doxorubicin-loaded amphiphilic polypeptide-based nanoparticles as an efficient drug delivery system for cancer therapy. *Acta Biomater.* **9**, 9330–9342 (2013).

89. Zhao, J., *et al*. Fabrication of hybrid nanostructures based on Fe_3O_4 nanoclusters as theranostic agents for magnetic resonance imaging and drug delivery. *Nanoscale Res. Lett.* **14**, (2019).

90. Hong, W. *et al.* A G2/M-phase specific drug delivery system based on increased exposure of phosphatidylethanolamine on mitotic cancer cells and low pH in tumor tissues. *J. Drug Deliv. Sci. Technol.* **52**, 224–235 (2019).

ANNEX A

Figures I to IX shows the equipments used during the experiments performed in this work.

Figure I – Peristaltic pump ISM 845, ISMATEC.

Figure II - Drying oven FD 115, Binder.

Figure III - Magnetic stirring plate IKA® C-MAG HS 7 with temperature control IKA® ETS-D5.

Figure IV - Centrifugal MPW-260R, MPW Med. Instruments.

Figure V – Analytical mill, IKA A11 basic.

Figure VI – Ultrasons-H, P-Selecta.

Figure VII - Vertical tubular furnace ROS 50/250/12, Thermoconcept.

Figure VIII - Orbital shaker IKA® KS 130 basic.

Figure IX - T70 UV-VIS spectrophotometer, PG Instruments Ltd.